Silk fibroin porous scaffolds by N_2O foaming

Devid Maniglio*, Walter Bonani, Claudio Migliaresi, Antonella Motta

Department of Industrial Engineering and BIOtech Research Centre, University of Trento, Trento, Italy,

*Corresponding author: via delle Regole 101, 38123 Trento, Italy. E-mail: devid.maniglio@unitn.it Tel +39 0461 282751

Abstract

Silk fibroin has acquired increasing interest for biomedical applications, and namely for the fabrication of scaffolds for tissue engineering, because of its highly positive biological interaction and the possibility to adapt the material to several application requirements by adopting different fabrication methods, in order to make films, sponges, fibers, nets or gels with predictable degradation times.

For tissue engineering, in most cases porous scaffolds are required, in some cases possibly *in situ* forming and therefore fabricated in mild body-compatible conditions.

In this work, we present a novel one-step method for the preparation of silk fibroin foams starting from water solutions and using low-pressure nitrous oxide gas as foaming agent. This foaming technique allows preparing fibroin porous scaffolds with easily tunable porosity, in mild processing conditions with the use of a relatively inert foaming agent saturating a fibroin water solution, that could be occasionally injected through a thin needle in the implantation site where expansion and foaming would occur.

Optimal foaming processing conditions have been investigated, and the prepared foams have been characterized with Fourier Transform Infrared Spectroscopy (FTIR) compressive mechanical and rheological properties measurements, and by scanning electron microscopy (SEM) and microCT.

Introduction

Silk fibroin has acquired in the last years increasing attention for applications in tissue engineering thanks to its noticeable biocompatibility and the possibility to tune its architecture and physical properties[1,2,3,4]. Fibroin molecules assembly capacity allows the realization of scaffolds in multiple forms: nets by electrospinning, films by casting, gels by using ultrasounds, acids, supercritical CO_2 or by the application of shear stresses, sponges by salt leaching and/or freeze drying starting from fibroin concentrated solutions or gels. [5,6]

Generally, a scaffold should be porous, with porosity and pore size tailored to allow cells penetration[7–11]. Porosity and pore size in the case of fibroin can been adjusted by modulating amount and size of the leachable particles in the case of salt leaching, or by using directional freeze-drying methods[12]. Sometimes freeze-drying is combined with salt leaching[2] to increase and control pores dimension, usually starting from concentrated fibroin-water solutions or gels.

To prepare polymeric porous scaffolds, gaseous porogens such as supercritical carbon dioxide ($scCO_2$) and nitrogen (N_2) can be used [13] However, use of N_2 is generally limited to polymer melt extrusion while $scCO_2$ foaming needs complex apparatuses due to the high pressures involved and doesn't allow pore size control. In addition, the chemical reactivity of the $scCO_2$ with the other components is sometimes not negligible and can cause unwanted modifications in the material.[14–18] In particular, the dissolution of CO_2 in water and its transformation in carbonic acid reduces pH, which can cause denaturation or precipitation of the suspended proteins because of the neutralization of the surface charge. In the case of fibroin, whose isoelectric point lays between pH 3.6 and pH 4.0, this phenomenon can occur at small carbonic acid concentration, leading to fast solution gelation[14–20].

Nitrous oxide (N_2O) is a gas highly soluble both in hydrophilic and in hydrophobic substances (Ostwald coefficient L= 0.4 for water, L=1.4 for fats at 37°C).[21] This peculiarity permits its dissolution in hydrophobic polymers, like lipids and phospholipids and in both hydrophobic and hydrophilic regions of proteins where the gas can accumulate. In fact, molar partition coefficient K for N_2O partitioning between water and olive oil ($N_2O_{\ WATER} \rightleftarrows N_2O_{\ OIL}$) is reported to be 2.97 [22,23]. N_2O has long been used as a general anesthetic and as a carrier for general anesthetic drugs; it is neither flammable nor toxic. Compared to CO_2, N_2O is relatively inert in water and does not induce pH modifications[24], moreover it has been reported to have bacteriostatic properties when pressurized [25].

In this paper, we describe a novel low-pressure single-step method for the preparation of fibroin constructs starting from silk fibroin water solutions and using N_2O as foaming agent. When pressurized, nitrous oxide readily dissolves in the fibroin solution and determines its expansion during the extrusion from a reservoir.

Usually, upon casting or extrusion fibroin constructs require additional stabilization procedures such as exposure to heat, water vapor or methanol solutions, to render them insoluble in water[26,27]. However, by properly tuning the foaming conditions, we obtained water stable fibroin foams without any additional stabilization procedure. In particular, while these treatments are necessary when foams are produced with the use of a larger nozzle, no other procedures are required when the extrusion is performed through a thin needle. This condition is in fact sufficient to allow the fabrication of stable fibroin foams.

The method can be easily to make porous scaffolds from a wide range of natural and synthetic polymers starting from their water suspension, including mixtures of them and allowing the easy incorporation of additives (like inorganic particles or bioactive molecules) just by tuning the initial water suspension composition.[28]

Experimental

Silk fibroin water solution

Silk fibroin was obtained from polyhybrid *Bombyx mori* white cocoons (Cooperativa Sociolario, Como, Italy). To remove sericin, cocoons were degummed in alkaline water baths at 98°C for 1.5 hours with 1.1 g/l and 0.4 g/l Na_2CO_3, respectively. Degummed silk was then washed several times in de-ionized (DI) water and dried at room temperature (RT) to obtain native silk fibroin fibers. Fibroin fibers were then dissolved in 9.3M LiBr (2 g of fibroin in 10 ml of LiBr solution) at 65°C for 2.5 hours [3]. The solution was then dialyzed against DI water for 3 days at RT in a Slide-A-Lyzer dialysis cassette (3.5K MWCO, Pierce, Rockford, IL, USA) to remove the LiBr salt and then filtered to remove impurities. 6% w/v silk fibroin water solution was finally recovered from dialysis and 5% and 2% w/v fibroin solutions were obtained by dilution with bi-distilled water.

Foaming apparatus

A stainless steel 0.5 liters (ICO, Whip it, Vancouver, Canada) siphon was used for foaming. Pressurization equal to 0.55 MPa or 1.1 MPa was achieved with standard 8 g N_2O cartridges (iSi GmbH, Austria). Investigated samples have been prepared by using two different purging nozzles, a larger one 10 mm inner diameter and 50 mm long, and a thinner needle 2 mm inner diameter, 100 mm long (see Fig. 1).

Foaming method

The method consisted of 4 main steps (as described in Fig. 1): initially, the siphon was loaded with the fibroin solution (5% or 2% w/v) and the container was pressurized with N_2O at 0.55 or 1.1 MPa (Fig. 1a and 1b); after 30 minutes to allow dissolution of N_2O (Fig. 1c), the container was set upside down and the solution was extruded through the nozzle/needle by opening the depressurizing valve (Fig. 1d). The expansion of the

dissolved gas caused the instantaneous foaming of the solution during its flow through the nozzle/needle.[29]

Foams prepared with the larger nozzle were unstable in water while foams obtained using the thin needle resulted to be water stable.

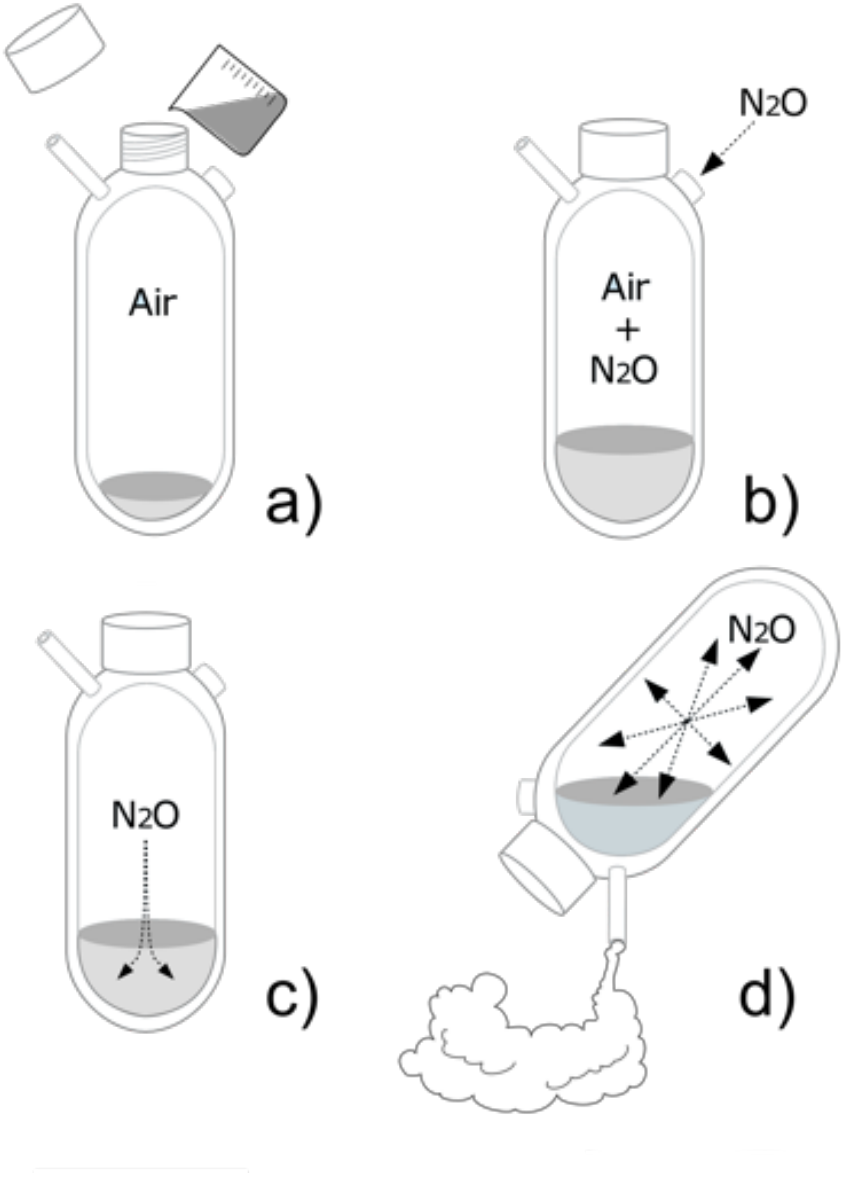

Fig. 1 Scheme of the foaming method: a) container loaded with fibroin aqueous solution; b) the container is pressurized with N2O at a predetermined pressure, c) the N2O is allowed to diffuse and solubilize into the solution, accumulating in the suspended protein d) the solution is expelled out of the container by opening a valve: the N2O expansion determines the solution extrusion through the nozzle and the fibroin foaming.

Evaluation of the foaming potential

The expansion capability of the starting solutions was evaluated using transparent cylinders (polyethylene terephthalate tubes, 90 mm height, 19 mm inner diameter) equipped with a valve-embedded cap (Fizz giz, High Point, NC, USA).

2 ml fibroin solution was loaded in the tube and pressurized at 0.55 and 1.1 MPa using a N_2O tank (Air Liquide, Italy) for 30 min. Foam expansion was estimated by direct measurement of the foam level inside the transparent bottle after controlled gas release.

The expansion ratio (η) was calculated as the ratio between the initial solution and the final foam volumes: $\eta = \frac{V_{Foam}}{V_{Initial\ solution}}$

Samples preparation

Fibroin aqueous solutions at 5% w/v and 2% w/v concentrations were foamed under different conditions to study their effect on the resulting foams and on the procedure itself. In particular, needle/nozzle geometry and size, and two initial N_2O pressure values (0.55 and 1.1 MPa) were considered.

Foams prepared with the large nozzle, which resulted soluble if exposed to water, required a post processing treatment which consisted in their freeze-drying followed by immersion in methanol/water solution (80:20 ratio, 10 minutes) to induce β-sheet fibroin molecular assembly.

On the contrary, foams obtained using the thin needle were water stable, wouldn't require any further stabilizing procedures. Some foams underwent straight to rheological characterization after production. However, to avoid collapse during drying, samples for electron microscopy, microCT and IR spectroscopy underwent to freeze-drying prior measurements.

IR spectra collected on the foams were compared with those of non-foamed freeze-dried 2% fibroin solution.

The complete list of used samples and of tested conditions is reported in **Errore. L'origine riferimento non è stata trovata.**.

Sample description	**Extrusion**	**N_2O Pressure [MPa]**	**Fibroin solution Concentration % w/v**	**Stabilization**
Silk Fibroin solution	No	No	2%	No
Silk Fibroin foam	10mm ø nozzle	0.55	2%	
		0.55	5%	
		1.1	2%	
		1.1	5%	
	10mm ø nozzle	0.55	2%	80:20 Methanol : Water
		0.55	5%	
		1.1	2%	
		1.1	5%	
	2mm ø, long needle	0.55	2%	No
		0.55	5%	
		1.1	2%	
		1.1	5%	

Table 1: list of all the materials prepared using different process variables: extrusion method, foaming pressure, solution concentration and post-treatment after freeze dry.

All the foams were produced at room temperature (22 ± 2 °C).

Samples characterization

SEM analysis has been performed on freze-dried fibroin foams after Pt/Pd sputtering with a Supra 40 scanning electron microscope (Carl Zeiss AG, Oberkochen, Germany) to evaluate morphology and estimate pores dimension. Micrographs were analyzed with ImageJ software (National Institutes of Health, Bethesda, MD, USA)[30].

FTIR-ATR Perkin Elmer Spectrum One in the spectral region of 1600-600 cm^{-1} was used to assess protein secondary structure, before and after stabilization. Data fitting on the 1700–1600 cm^{-1} spectral region was performed following the procedure suggested by Hu *et al.* and *Callone et al.*[26,31] in order to estimate the contribution of random coil, α-helices, β-turns and β-sheets structures to the amide I peak.

Compressive mechanical properties were performed on the larger nozzle prepared freeze-dried foams while the foams prepared by using the thin needle underwent to rheological tests. Mechanical compressive tests were performed on foams in dry and wet conditions after methanol stabilization by using a Universal Testing Machine model ElectroForce3200 (Bose, MN, USA), equipped with a 225 N load cell. Tests were performed on parallelepiped shape cut samples with base area equal to 90 ± 10 mm^2 and height equal to 3.0 ± 0.5 mm. For each foaming condition 5 samples were used. Compression tests were carried out under displacement control with a speed of 2 mm/sec at room temperature in case of dry samples (25% Relative Humidity) and 37°C in case of hydrated samples. Afterwards, elastic modulus was calculated from the slope of the initial portion of the stress-strain curve (between 0.5 and 2.5% deformation) to identify the initial stiffness of the material at small deformations in the linear elastic regime. Compressive stress value at 50% deformation was also evaluated as a measure of material compression strength.

Rheological characterization of the as prepared fibroin foams obtained by extrusion through the thin needle, was performed using a HR-2 Discovery Hybrid Rheometer (TA Instruments, DE, USA) equipped with 40 mm parallel plates with cross hatched surface. Fibroin foams were extruded on a 6 cm Petri dish, collected with a spatula and laid carefully on the lower plate of the rheometer. The upper plate was lowered to meet the foam surface; samples were pre-loaded to 0.5 N and sample thickness was recorded (typically 2 mm). Foams were tested in an oscillatory time sweep mode at 37°C with 5%

constant oscillatory deformation and a frequency of 1 Hz for a total of 180 sec.

Foams structure was investigated using Skyscan 1176 *in-vivo* microCT (Bruker, Belgium, 9 µm resolution, 40 kV, 600 uA, no filter and 0.3°rotation step size), after immersion in 10% Lugol's iodide solution for 30 min, used as a contrast agent. 3D reconstructions, porosity calculation and 3D rendering were performed respectively with NRecon, CT-analyser and CTVox softwares developed by Bruker. Porosity was calculated as the ratio between empty and total sample volume and where compared to values obtained with by a slightly modified n-hexane displacement method[32,33]. The scaffolds were dried at 65°C overnight in vacuum, weighed, and then immersed in hexane for 30 min to allow full imbibition. The hexane-impregnated scaffolds were weighted (W_{HEX}). Empty volume (occupied by hexane) and fibroin volume were calculated from the respective weight measurement and density value as: $V_{FN} = W_{FN}\, \rho_{FN}$ and $V_{HEX} = W_{HEX}\, \rho_{HEX}$, with ρ_{FN} = 1.348 g/cm^3 and ρ_{HEX} =0.6558 g/cm^3 (T=25°C).

Mold preparation for simulated injection tests in cavity

A mold in poly-dimethylsiloxane rubber was realized to simulate a body cavity and the possibility to realize in-situ foaming. The mold was realized pouring Sylgard 184®, a low viscosity poly-dimethylsiloxane (PDMS, Dow Corning) into a 50 ml Falcon tube containing a 25 mm diameter polypropylene sphere. PDMS cross-linking was obtained by overnight thermal curing at 150°C, then the sphere was removed leaving its spherical print in the transparent rubber cylinder.

Results and discussion

Foaming potential of different fibroin solutions was evaluated by estimating the volume increase of the previously pressurized fibroin solution after degassing in a transparent tube. The calculated expansion coefficient η allows evaluating the correlation between the volumetric increase due to depressurization and the main process variables (gas pressure and fibroin concentration). Data reported in **Table 2** evidence a direct correlation between η and the pressure values, and an inverse correlation with the solution concentration, probably due to the increase of the viscosity that hinders the gas expansion.

Concentration	2%		5%	
Pressure [MPa]	0.55	1.1	0.55	1.1
η (exp. coeff.)	3.5±0.3	7.0±0.5	2.1±0.3	4.6±0.5

Table 2 Expansion ratio η calculated by evaluation of the expansion volume of 2 ml solutions at 2% and 5% in pressurized tubes.

Foams produced with large nozzle

Fibroin foams obtained using the siphon with the large nozzle at initial N_2O pressure of 0.55 and 1.1 MPa were stable for about 15 minutes after the extrusion, then bubbles started coalesce and the foams tended to collapse. For this reason, foams were freeze-dried, immersed in methanol-water solutions (80:20 volume ratio) for 5 minutes and then abundantly rinsed with DI water to prepare water stable foams.

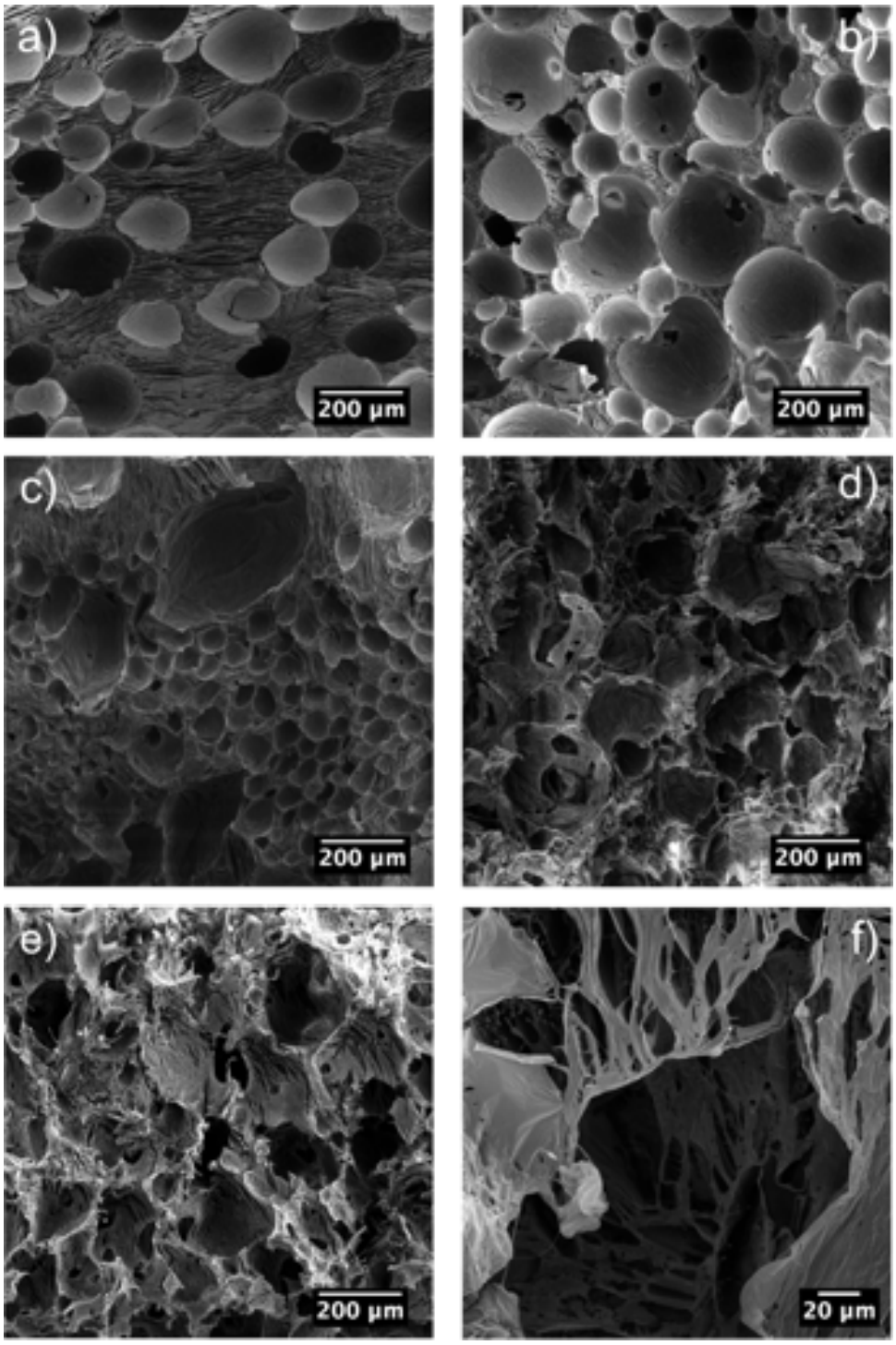

Fig. 2 SEM image of the foams obtained with the large nozzle (10 mm inner diameter) from different fibroin solutions and N_2O pressure: a) 5% at 0.55 MPa; b) 5% at 1.1 MPa; c) 2% 0.55 MPa; d) 2% at 1.1 MPa; e) 5% and 1.1 MPa after methanol treatment: the breakage of the walls of the pores is evident; f) detail of the pore structure.

Pore size and distribution was evaluated from SEM images (Fig 2a-d) and microCT (Fig. 3). As a general rule, higher N_2O pressures and lower fibroin solution concentration

resulted in foams with bigger and higher density pores. Foams obtained starting from 5% fibroin concentration and pressurized at 0.55 MPa are constituted by an arrangement of spherical holes, resulting from the N_2O bubbles expansion, with diameters ranging from 100 to 300 μm. Both SEM and microCT pictures evidenced the presence of pore throats that allow communication among adjacent cavities. Pore walls appeared to be intercalated by elongated lamellar structures, typically obtained when standard fibroin solutions withstand freeze-drying. At higher N_2O pressure (1.1 MPa) the overall structure of the foam is maintained: pores are more closely packed and their size shifts to larger dimension (100 to 400 μm).

Foams made from fibroin solution at 2% exhibit similar pore size distribution, from 100 to 300 μm at 0.55 MPa that broadens up to 600 μm at 1.1 MPa, as consequence of the reduction of the solution viscosity.

After exposure to methanol/water solution for fibroin stabilization, open porosity is widely improved due to β-sheet formation, causing overall material shrinkage and the rupture of the thin pores walls that limit the communication between the cavities (Fig 2e and 2f).

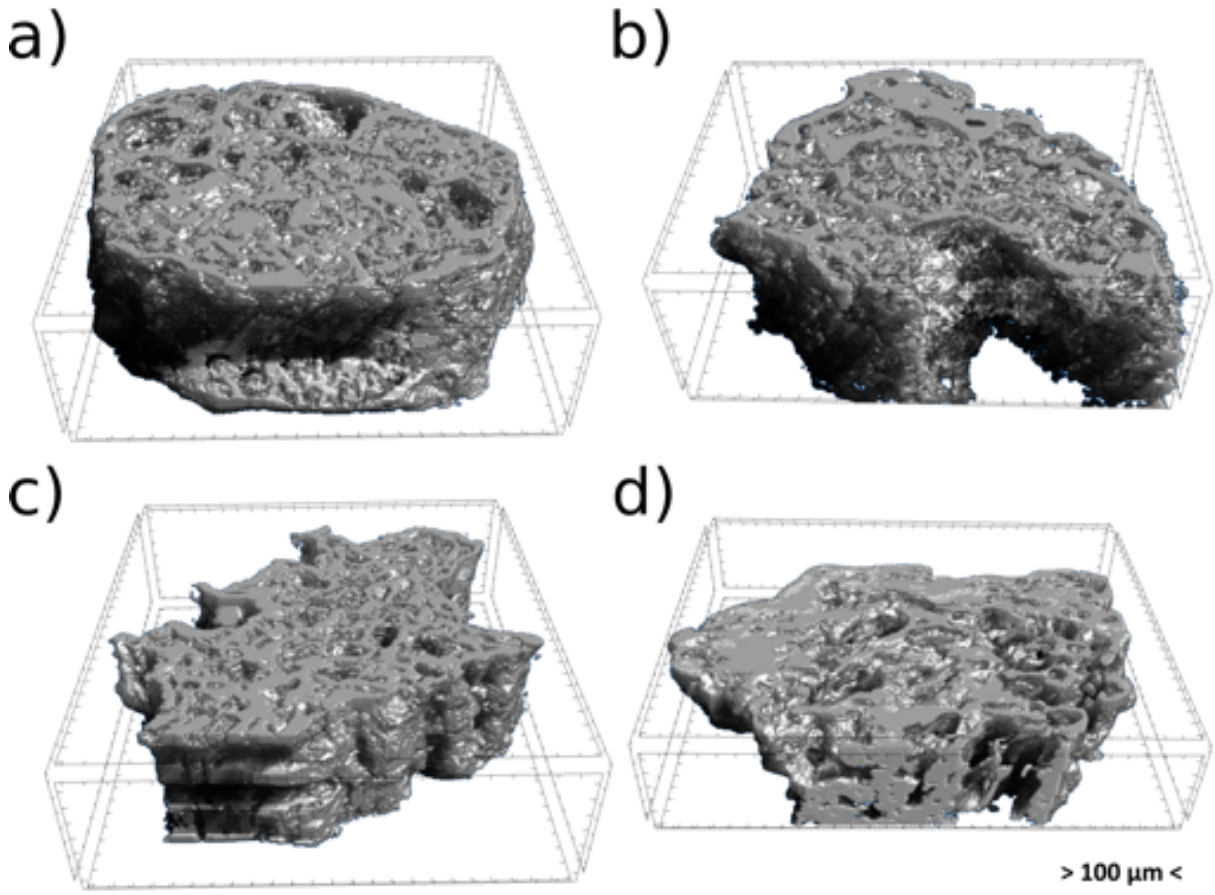

Fig. 3 MicroCT structure reconstruction of foams obtained at different fibroin solution concentration and N_2O pressure: a) 2% w/v and 0.55 MPa; b) 2% w/v and 1.1 MPa; c) 5% w/v and 0.55 MPa; d) 5% w/v and 1.1 MPa.

Samples were evaluated using n-hexane displacement method to assess their porosity. The measured values were all accumulating in the range from 92% to 94% (± 1%) for fiborin concentrations of 5% and 2% respectively, independently from the pressure applied. These values, together with the presence of large cavities, are in the range of those reported in literature for scaffolds made of fibroin and proposed for possible application for bone tissue engineering [2,8,34]. Nevertheless, n-hexane displacement method is sensitive to all the sample porosity (even the smaller in size), which comes from the volume occupied by the water present in the fibroin solution, removed by to freeze-drying process. Porosity values calculated on not foamed fibroin solutions (5% and 2%)

underwent to freeze-dry, resulted equal to be 78% and 85% (± 1%) respectively. This makes the n-hexane displacement method not enough sensitive to evidence the contribution to big pores content due to gas expansion and correlated to gas pressure and solution concentration.

The microCT apparatus used for this characterization, having a resolution limit of 9 μm, is intrinsically blind to pores smaller than this value. This makes the porosity data obtained with this technique, even if not representative of the whole porosity, more sensitive to cavities wider than 9 μm and, thus, more suitable for a direct correlation between porosity value higher than 9μm ($\boldsymbol{P}_{>9\mu m}$) and process parameters.

$\boldsymbol{P}_{>9\mu m}$ calculated from microCT volume reconstruction (Table 3) range from 46.6% to 52.2%, tend to increase with the N_2O pressure and to decrease with the concentration of the solution. This behavior is in agreement with the trend of the expansion ratio μ, in which lower concentrated and less viscous solutions displayed higher expansion potential.

As discussed in the following, porosity for the small needle made foams are generally larger.

	Total porosity	
Foaming parameters	**Large nozzle**	**Small needle**
2% and 0.55 MPa	46.6%	49.5%
2% and 1.1 MPa	52.2%	53.3%
5% and 0.55 MPa	43.0%	67.7%
5% and 1.1 MPa	45.6%	73.6%

Table 3 Porosity values ($P_{>9\mu m}$) calculated from microCT scans on the different foams produced from large nozzle and small needle after freeze dry

Structural changes in the fibroin foams after the different processes were evidenced by FTIR-ATR analysis and compared with a not processed freeze-dried fibroin solution (Fig. 4). Here we report FTIR spectra obtained using 5% fibroin solution at 1.1 MPa, as representative for all the other foaming conditions, which didn't show significant differences.

The infrared spectral region within 1700–1500 cm^{-1}, which refer to absorption of the peptide backbones of amide I (1700–1600 cm^{-1}) and amide II (1600–1500 cm^{-1}), are commonly used for the analysis of different secondary structures of silk fibroin[35]. Amide I band in not processed freeze-dried fibroin solution showed a strong peak at 1644 cm^{-1}, which corresponds to a high contribution of random coil structures. The extrusion through a nozzle and the following treatment with methanol solution produced an evident shift of the amide I peak to 1622 cm^{-1} and the contemporary reduction of the 1539 cm^{-1} amide II peak, index of the increase of β-sheet structures.

The behavior is confirmed also by data fitting (Fig. 5) where it is evident a slight increase in β-sheet content, passing from 24.1% for the untreated freeze-dried solution to 32.7% in the foams extruded through the nozzle, with the contemporary reduction in α-helices and β-turns content (12.3% to 10.9% and 27.2% to 21.4% respectively). The exposure to methanol strongly emphasizes the β-sheet transition (35.9%), which is the reason of foam stabilization.

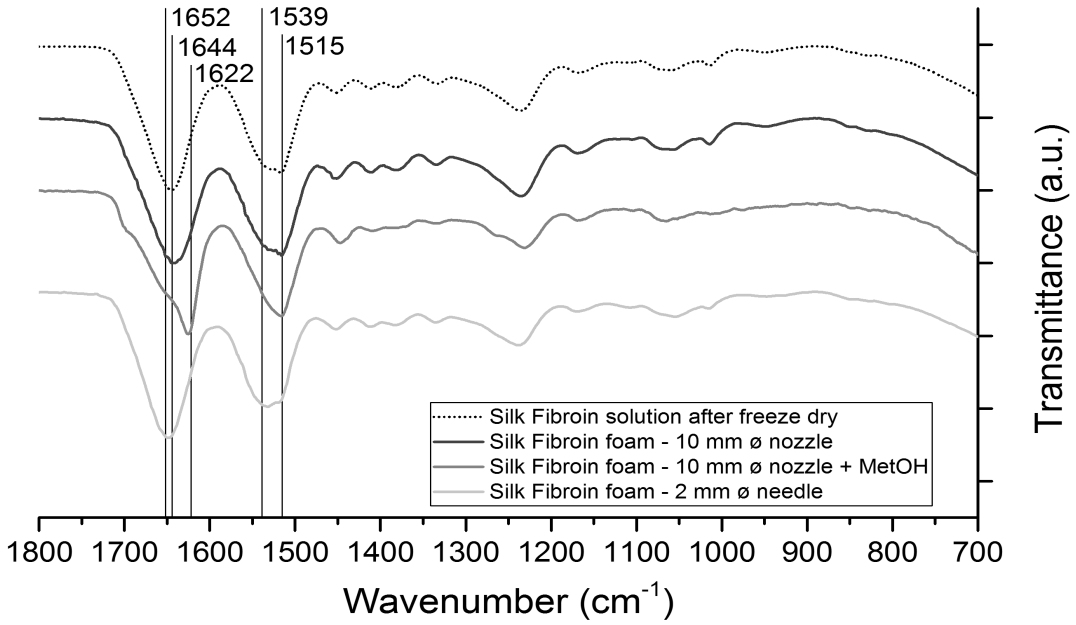

Fig. 4 Infrared spectra of freeze-dried fibroin foams obtained by gas foaming of fibroin solutions at 5% concentration and 1.1 MPa pressure through large nozzle (10 mm ø) and through thin needle (2 mm ø). The spectra are representative for all the other foaming conditions used. The spectrum of freeze-dried unprocessed fibroin solution is reported for comparison.

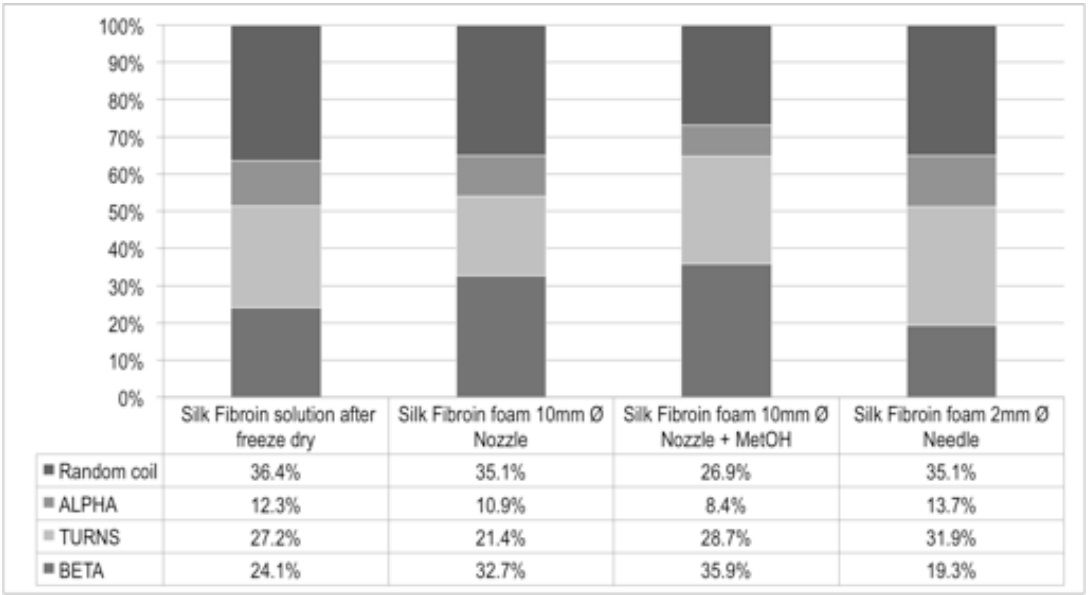

	Silk Fibroin solution after freeze dry	Silk Fibroin foam 10mm Ø Nozzle	Silk Fibroin foam 10mm Ø Nozzle + MetOH	Silk Fibroin foam 2mm Ø Needle
Random coil	36.4%	35.1%	26.9%	35.1%
ALPHA	12.3%	10.9%	8.4%	13.7%
TURNS	27.2%	21.4%	28.7%	31.9%
BETA	24.1%	32.7%	35.9%	19.3%

Fig. 5 Relative contributions of random coil, α-helix, β-turns and β-sheet structures obtained by peak fitting of amide I FTIR spectra on freeze-dried fibroin foams obtained by gas foaming of fibroin solutions at 5% concentration and 1.1MPa pressure through large nozzle (10 mm inner diameter) and through thin needle (2 mm inner diameter), compared with a freeze dried unprocessed fibroin solution. The spectra are representative for all the other foaming conditions used.

All the foams (0.55 and 1.1 MPa pressure, 2% and 5% solution concentration) after stabilization with methanol and freeze-drying were tested in compression to evaluate mechanical properties. In Fig. 6a and 7c representative curves are reported for dry and hydrated foams, respectively; while in Fig. 6b and 7d the values of the elastic modulus and compressive strength of the samples at 50% deformation are reported.

In dry conditions, the elastic modulus of the foams ranges between 40 kPa to 90 kPa. In general, foams prepared from 2% fibroin concentration presented lower elastic modulus and mechanical strength when compared to the higher concentration counterparts. However, the foams prepared from 5% solution and 1.1 MPa recorded an elastic modulus not different from the 2% foams. These results indicates that both stiffness and strength of the foams increase with the concentration of the starting solutions, but also that the stiffness of the foams can be decreased in consequence of higher working pressures. On the other side, the sample prepared starting from higher concentrated solution (5%) and lower expansion pressure (0.55 MPa) showed the highest values for the elastic modulus and compressive strength at 50% deformation between all the groups.

Wet samples, as expected, exhibit much lower modulus values due to the plasticizing effect of water. All the values are confined in the range between 3 kPa and 9 kPa, resulting in negligible differences among the samples.

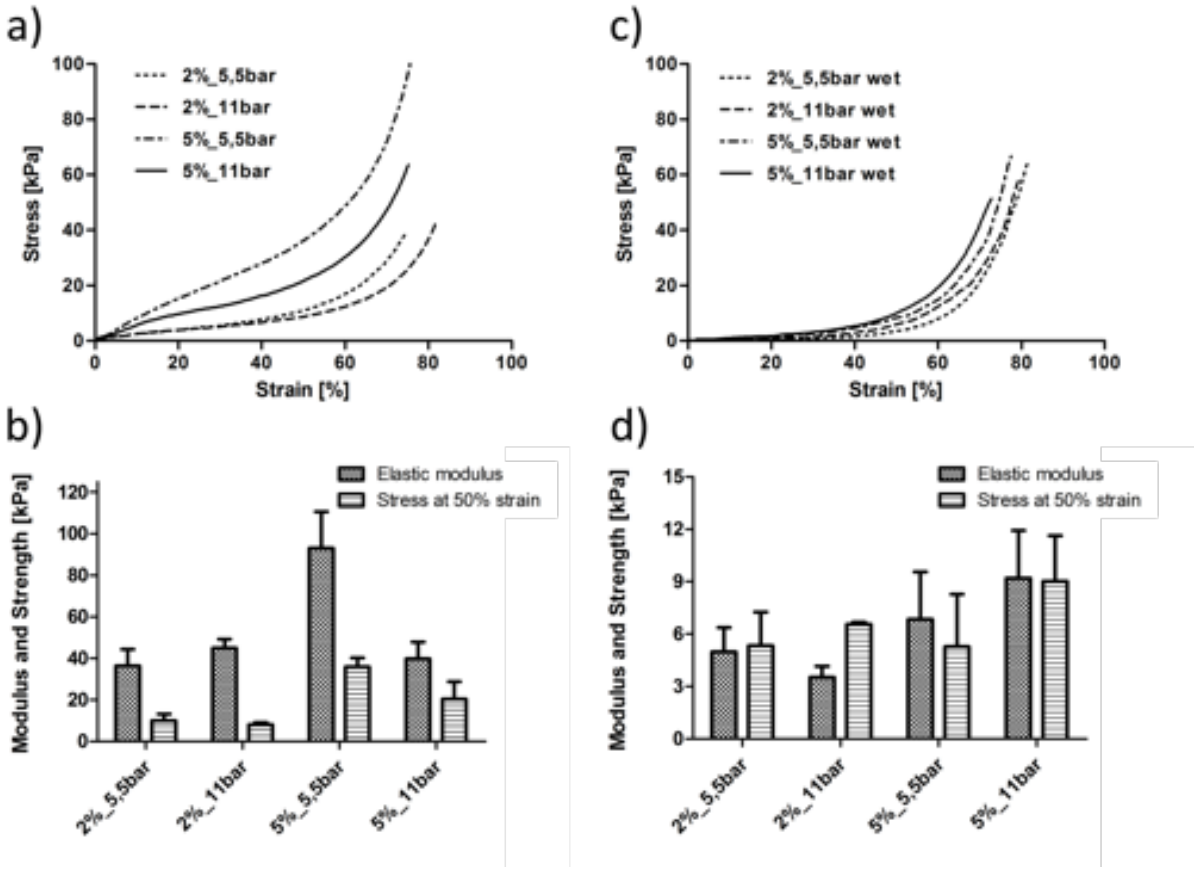

Fig. 6 Typical compression curves (up) and summary of the compression tests (down: elastic modulus and stress at 50% deflection) performed on dry (left) and wet (right) fibroin foam samples after freeze dry and methanol treatment.

Foams produced with small needle

When foams extrusion was performed through a thin needle (2 mm Ø, 100mm long) a significant different behavior was observed. These conditions allowed obtaining foams showing increased and connatural water stability, with a continuous wire-like porous microstructure (Fig. 7a). These foams did not require any further physical/chemical post-treatment, at the point that the direct extrusion in water bath didn't evidence fibroin re-suspension and loss of shape stability (Fig. 7a inset). This fact could be attributed to the shear forces produced during extrusion through the long needle that increase fibroin

crystallinity, as was already reported for fibroin in particular cases in literature [36,37,38]. The fibroin molecules assembly was confirmed by the FTIR analysis, which shows a shift of the amide I peak to 1652 cm^{-1} and the enhancement of the 1539 cm^{-1} peak in the amide II region, which is attributed to the increase of helix-like and β-turns structures (Fig. 4).[35,39,40]

Peak fitting on amide I region confirms the significant difference existing between the final foams obtained by extrusion through large nozzle or small needle, with helix-like and β-turns structures increasing from 10.9% to 13.7% and from 21.4% to 31.9 % respectively (Fig. 5).

As a result of this molecular arrangement foams produced following this procedure are capable to maintain a stable shape in water with no further treatment, even after several months of immersion in DI water.

Pore size of foams obtained at 5% concentration at 1.1 MPa (Fig. 7) is substantially in agreement with data for the larger nozzle extruded foams, while porosity raises up to 70% (Table 3 and Fig. S1). A larger fibroin molecules assembly, already evidenced in the FTIR analysis, can be also revealed from electron microscopy with the comparison of a fibrillar structure intercalating the big cavities and presenting an evident alignment in the direction of extrusion.

When the solution concentration is reduced to 2%, the pore size increased, in some cases up to 500 μm, as evincible in Fig. 7c. Also in this case a fibrillar structure is evident (Fig. 7d), even if fibers alignment is less appreciable. The obtained foam resulted stable with time, without collapse and loss of structure or significant change in shape if exposed to water. Infrared spectrum is identical to that shown in (Fig. 5), which confirms the enrichments in α-helix structures.

Formulations obtained with 2% concentration and 1.1 MPa pressure were considered suitable for exploring the possibility of using gas extrusion foaming to *in-situ* fill cavities with a “one-step” procedure. The test was performed using a PDMS mold containing a 25 mm diameter spherical cavity. By using the small diameter needle the foam was successfully injected, as reported in Fig. 7e into the PDMS cavity and was capable to completely fill the entire hollow cavity.

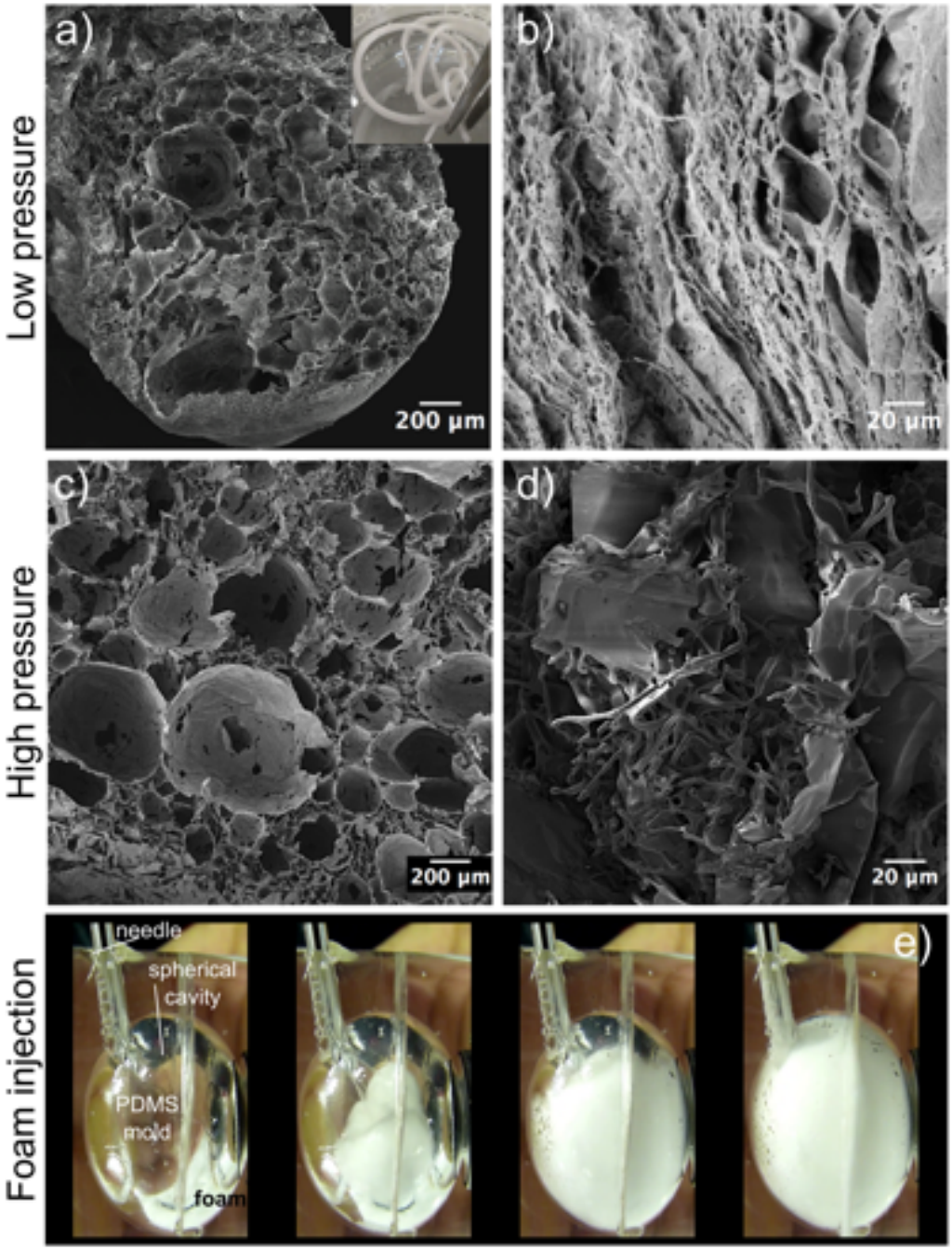

Fig. 7 a) SEM micrograph of water-stable fibroin foam extruded through small diameter needle (1.1 MPa and 5% protein concentration). Inset: evidence of wire-like structure; b) detail of the alignment of the fibrous structure derived from shear stresses generated by extrusion through the thin needle c) SEM micrograph of water-stable fibroin foam extruded through small diameter needle (1.1 MPa and 2% protein concentration). d) Evidence of the fibrillar structure after extrusion through the thin needle at low concentration (2%) e) Image sequence of 2% fibroin solution foam injection using a thin needle into a PDMS mold presenting a spherical cavity.

Rheological tests performed on the thin needle 4 different foams (Fig. 8) showed compatible values of G' and G'' for the samples produced after pressurization at 0.55 MPa, standing at about 200 Pa, with samples obtained from 2% fibroin concentration almost negligibly higher in values than those from 5%. Differently foams produced after pressurization at 1.1 MPa evidenced a sensible increase of G' value that passes from 850 Pa for solutions at low concentration to 1500 Pa for those at higher concentration, with the G'' loss modulus in both cases standing at about 200 Pa. These values are an indirect confirmation of the fact that shear stress plays an important role in fibroin structuring.

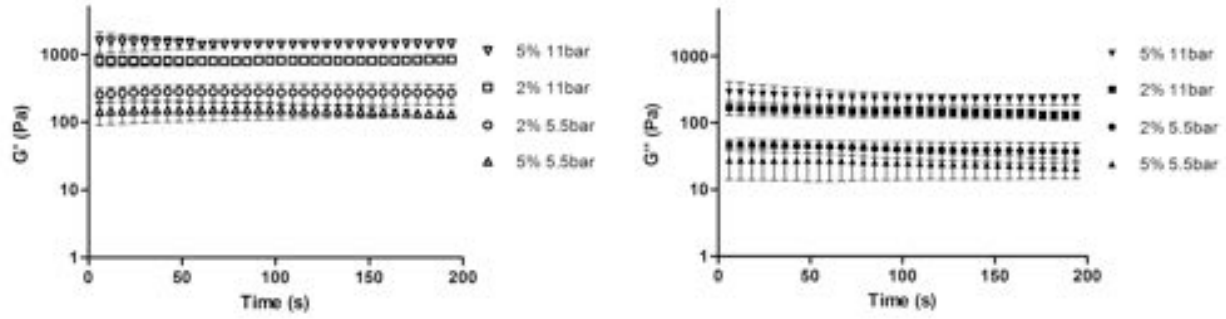

Fig. 8 Storage and loss modulus plots collected from rheological tests on foams obtained from 2% and 5% fibroin solutions after pressurization at 0.55 and 1.1 MPa.

Conclusion

We presented a one-step foaming technique that allows obtaining foams starting from silk fibroin suspended in aqueous solution by using the combination of pressured nitrous oxide gas extrusion through a nozzle or a small diameter needle. The technique exploits the high solubility of N_2O both into water and the protein, allowing fibroin expansion and, consequently, foaming.

Compared with other methods, the use of N_2O permits to obtain fibroin foams at room temperature and at moderate pressure level (about 1 MPa); particularly N_2O, if compared to other gases like CO_2, doesn't alter the pH of the solution, whose drop could protein gelation, precipitation or degradation.

Foams obtained using the large nozzle showed limited shape stability in the time, so requiring freeze-drying and exposure to methanol/water solution for stabilization. These foams were characterized by high trochlear porosity with pores dimensions directly correlated to the gas pressure and inversely correlated with the initial protein concentration.

Conversely, foams obtained using a small caliber needle (2 mm diameter) demonstrated an intrinsic chemical and structural stability towards water, directly after extrusion, thus not requiring further stabilization treatments. The shear stresses generated during the extrusion in the thin needle induced protein structuring in helix-like and β-turns forms simultaneously with the foaming expansion.

This one-step foaming procedure was also successfully tested for possible direct *in situ* injection, evidencing the potentiality of the foams produced in this way to completely fill even large cavities.

Based on these observations the proposed method is suitable for a possible direct application in a deficient body site with a minimal invasive procedure, allowing to produce and to inject *in situ* a stable fibroin foam as a porous bioactive degradable filler to support tissue regeneration (i.e. in a critical bone defect).

Acknowledgements

The authors are grateful to Dr. Sandra Schneider and prof. Martijn van Griensven from Experimental Trauma Surgery, Technical University of Munich, Germany, for the microCT measurements.

References

(1) Altman, G. H.; Diaz, F.; Jakuba, C.; Calabro, T.; Horan, R. L.; Chen, J.; Lu, H.; Richmond, J.; Kaplan, D. L. Silk-Based Biomaterials. *Biomaterials* **2003**, *24*, 401–416.

(2) Nazarov, R.; Jin, H.-J.; Kaplan, D. L. Porous 3-D Scaffolds from Regenerated Silk Fibroin. *Biomacromolecules* **2004**, *5*, 718–726.

(3) Motta, A.; Maniglio, D.; Migliaresi, C.; Kim, H.; Wan, X.; Hu, X.; Kaplan, D. L. Silk Fibroin Processing and Thrombogenic Responses. *J. Biomater. Sci. Polym. Ed.* **2009**, *20*, 1875–1897.

(4) Maniglio, D.; Bonani, W.; Bortoluzzi, G.; Servoli, E.; Motta, A.; Migliaresi, C. Electrodeposition of Silk Fibroin on Metal Substrates. *J. Bioact. Compat. Polym.* **2010**, *25*, 441–454.

(5) Rockwood, D. N.; Preda, R. C.; Yücel, T.; Wang, X.; Lovett, M. L.; Kaplan, D. L. Materials Fabrication from Bombyx Mori Silk Fibroin. *Nat. Protoc.* **2011**, *6*, 1612–1631.

(6) Motta, A.; Foss, C.; Migliaresi, C. Tailoring Silk-Based Matrices for Tissue Regeneration. In *Tailored Polymer Architectures for Pharmaceutical and Biomedical Applications*; pp. 281–299.

(7) Murphy, C. M.; Haugh, M. G.; O'Brien, F. J. The Effect of Mean Pore Size on Cell Attachment, Proliferation and Migration in Collagen–glycosaminoglycan Scaffolds for Bone Tissue Engineering. *Biomaterials* **2010**, *31*, 461–466.

(8) Karageorgiu, V.; Kaplan, D. Porosity of 3D Biomaterial Scaffolds and Osteogenesis. *Biomaterials* **2005**, *26*, 5474–5491.

(9) Alali, A. S.; Fowler, R. A.; Mainprize, T. G.; Scales, D. C.; Kiss, A.; de Mestral, C.; Ray, J. G.; Nathens, A. B. Intracranial Pressure Monitoring in Severe Traumatic Brain Injury: Results from the American College of Surgeons Trauma Quality Improvement Program. *J. Neurotrauma* **2013**, *30*, 1737–1746.

(10) Bonfield, W. Designing Porous Scaffolds for Tissue Engineering. *Philos. Trans. R. Soc. A Math. Phys. Eng. Sci.* **2006**, *364*, 227–232.

(11) Wang, Y.; Bella, E.; Lee, C. S. D.; Migliaresi, C.; Pelcastre, L.; Schwartz, Z.; Boyan, B. D.; Motta, A. The Synergistic Effects of 3-D Porous Silk Fibroin Matrix Scaffold Properties and Hydrodynamic Environment in Cartilage Tissue Regeneration. *Biomaterials* **2010**, *31*, 4672–4681.

(12) Zhang, H.; Cooper, A. ?I. Aligned Porous Structures by Directional Freezing. *Adv. Mater.* **2007**, *19*, 1529–1533.

(13) *Biomedical Foams for Tissue Engineering Applications*; Netti, P. A., Ed.; Elsevier Science, 2014.

(14) Liao, X.; Zhang, H.; He, T. Preparation of Porous Biodegradable Polymer and Its Nanocomposites by Supercritical CO 2 Foaming for Tissue Engineering. *J. Nanomater.* **2012**, *2012*, 1–12.

(15) Jacobs, L. J. M.; Kemmere, M. F.; Keurentjes, J. T. F. Sustainable Polymer Foaming Using High Pressure Carbon Dioxide: A Review on Fundamentals, Processes and Applications. *Green Chem.* **2008**, *10*, 731.

(16) Dehghani, F.; Annabi, N. Engineering Porous Scaffolds Using Gas-Based Techniques. *Curr. Opin. Biotechnol.* **2011**, *22*, 661–666.

(17) Christenson, E. M.; Soofi, W.; Holm, J. L.; Cameron, N. R.; Mikos, A. G. Biodegradable Fumarate-Based polyHIPEs as Tissue Engineering Scaffolds. *Biomacromolecules* **2007**, *8*, 3806–3814.

(18) Mooney, D. J.; Baldwin, D. F.; Suh, N. P.; Vacanti, J. P.; Langer, R. Novel Approach to Fabricate Porous Sponges of poly(D,L-Lactic-Co-Glycolic Acid) without the Use of Organic Solvents. *Biomaterials* **1996**, *17*, 1417–1422.

(19) Harris, M. The Isoelectric Point of Silk. *Bur. Stand. J. Res.* **1032**, *9*, 557.

(20) Sookne, A. M.; Harris, M. Electrophoretic Studies of Silk. *Text. Res.* **1939**, *9*, 374–383.

(21) Young, C. L. Oxides of Nitrogen (Solubility Data Series). *The Journal of Chemical Thermodynamics*, 1982, *12*, 1–369.

(22) Pinnick, E. R.; Erramilli, S.; Wang, F. The Potential of Mean Force of Nitrous Oxide in a 1 , 2-Dimyristoylphosphatidylcholine Lipid Bilayer. *Chem. Phys. Lett.* **2010**, *489*, 96–98.

(23) Steward, A.; Allott, P. R.; Cowles, A. L.; Mapleson, W. W. Solubility Coefficients for Inhaled Anaesthetics for Water, Oil and Biological Media. *Br. J. Anaesth.* **1973**, *45*, 282–293.

(24) O'Neil, M. J. *The Merck Index an Encyclopedia of Chemicals, Drugs, and Biologicals*; 13th ed.; Whitehouse Station, N.J Merck, 2001.

(25) Thom, S. R.; Marquis, R. E. Microbial-Growth Modification By Compressed Gases and Hydrostatic-Pressure. *Appl. Environ. Microbiol.* **1984**, *47*, 780–787.

(26) Hu, X.; Kaplan, D.; Cebe, P. Determining Beta-Sheet Crystallinity in Fibrous Proteins by Thermal Analysis and Infrared Spectroscopy. *Macromolecules* **2006**, *39*, 6161–6170.

(27) Boulet-Audet, M.; Lefèvre, T.; Buffeteau, T.; Pézolet, M. Attenuated Total Reflection Infrared Spectroscopy: An Efficient Technique to Quantitatively Determine the Orientation and Conformation of Proteins in Single Silk Fibers. *Appl. Spectrosc.* **2008**, *62*, 956–962.

(28) Maniglio, D.; Bonani, W. Method for Manufacturing Porous Scaffolds for Biomedical Uses and Scaffolds Thereof. WO 2016046715 A1, 2016.

(29) Maniglio, D.; Bonani, W. Procedimento per La Realizzazione Di Scaffold Porosi per Usi Medicali E Relativi Scaffold. 1427718, 2014.

(30) Rasband, W. S. ImageJ. US National Institutes of Health, Bethesda, MD, 1997.

(31) Callone, E.; Dirè, S.; Hu, X.; Motta, A. Processing Influence on Molecular Assembling and Structural Conformations in Silk Fibroin: Elucidation by Solid-State NMR. *ACS Biomater. Sci. Eng.* **2016**, *2*, 758–767.

(32) Gil, E. S.; Kluge, J. A.; Rockwood, D. N.; Rajkhowa, R.; Wang, L.; Wang, X.; Kaplan, D. L. Mechanical Improvements to Reinforced Porous Silk Scaffolds. *J. Biomed. Mater. Res. Part A* **2011**, *99A*, 16–28.

(33) Nazarov, R.; Jin, H.-J.; Kaplan, D. L. Porous 3-D Scaffolds from Regenerated Silk Fibroin. *Biomacromolecules* **2004**, *5*, 718–726.

(34) Akay, G.; Birch, M. A.; Bokhari, M. A. Microcellular polyHIPE Polymer Supports Osteoblast Growth and Bone Formation in Vitro. *Biomaterials* **2004**, *25*, 3991–4000.

(35) Lu, Q.; Hu, X.; Wang, X.; Kluge, J. a.; Lu, S.; Cebe, P.; Kaplan, D. L. Water-Insoluble Silk Films with Silk I Structure. *Acta Biomater.* **2010**, *6*, 1380–1387.

(36) Xie, F.; Zhang, H.; Shao, H.; Hu, X. Effect of Shearing on Formation of Silk Fibers from Regenerated Bombyx Mori Silk Fibroin Aqueous Solution. *Int. J. Biol. Macromol.* **2006**, *38*, 284–288.

(37) Rössle, M.; Panine, P.; Urban, V. S.; Riekel, C. Structural Evolution of Regenerated Silk Fibroin under Shear: Combined Wide- and Small-Angle X-Ray Scattering Experiments Using Synchrotron Radiation. *Biopolymers* **2004**, *74*, 316–327.

(38) Xie, F.; Zhang, H.; Shao, H.; Hu, X. Effect of Shearing on Formation of Silk Fibers from Regenerated Bombyx Mori Silk Fibroin Aqueous Solution. *Int. J. Biol. Macromol.* **2006**, *38*, 284–288.

(39) Jin, H.-J.; Kaplan, D. L. Mechanism of Silk Processing in Insects and Spiders. *Nature* **2003**, *424*, 1057–1061.

(40) He, S.; Valluzzi, R.; Gido, S. P. Silk I Structure in Bomyx Mori Silk Foams. *Int. J. Biol. Macromol.* **1999**, *24*, 187–195.